



Observation of new resonances in the $\Lambda_b^0 \pi^+ \pi^-$ system

LHCb collaboration[†]

Abstract

We report the observation of a new structure in the $\Lambda_b^0 \pi^+ \pi^-$ spectrum using the full LHCb data set of pp collisions, corresponding to an integrated luminosity of 9 fb^{-1} , collected at $\sqrt{s} = 7, 8$ and 13 TeV . A study of the structure suggests its interpretation as a superposition of two almost degenerate narrow states. The masses and widths of these states are measured to be

$$\begin{aligned}
 m_{\Lambda_b(6146)^0} &= 6146.17 \pm 0.33 \pm 0.22 \pm 0.16 \text{ MeV}, \\
 m_{\Lambda_b(6152)^0} &= 6152.51 \pm 0.26 \pm 0.22 \pm 0.16 \text{ MeV}, \\
 \Gamma_{\Lambda_b(6146)^0} &= 2.9 \pm 1.3 \pm 0.3 \text{ MeV}, \\
 \Gamma_{\Lambda_b(6152)^0} &= 2.1 \pm 0.8 \pm 0.3 \text{ MeV},
 \end{aligned}$$

with a mass splitting of $\Delta m = 6.34 \pm 0.32 \pm 0.02 \text{ MeV}$, where the first uncertainty is statistical, the second systematic and the third derives from the knowledge of the mass of the Λ_b^0 baryon. The measured masses and widths of these new excited states suggest their possible interpretation as a doublet of $\Lambda_b(1D)^0$ states.

Published in Phys. Rev. Lett. **123**, 152001 (2019).

© 2020 CERN for the benefit of the LHCb collaboration, CC-BY-4.0 licence.

[†]Authors are listed at the end of this Letter.

In the constituent quark model [1,2], baryons containing a beauty quark form multiplets according to the internal symmetries of flavour, spin, and parity [3]. Beyond the Λ_b^0 baryon, which is the lightest beauty baryon, a rich spectrum of radially and orbitally excited states is expected at higher masses. Several new baryon states have been discovered in recent years [4–8]. The spectrum of excited states decaying to the $\Lambda_b^0\pi^+\pi^-$ final state has already been studied by the LHCb experiment with the discovery of two narrow states [4], denoted $\Lambda_b(5912)^0$ and $\Lambda_b(5920)^0$. The heavier of these states was later confirmed by the CDF collaboration [9]. Mass predictions for the ground-state beauty baryons and their orbital and radial excitations are given in many theoretical works, *e.g.*, [10–13]. In addition to the already observed doublet of first orbital excitations, more states are predicted in the mass region near or above 6.1 GeV.¹

In this Letter, we document the study of the $\Lambda_b^0\pi^+\pi^-$ spectrum (charge conjugation is implied throughout this article) in the extended mass region between 6.10 and 6.25 GeV, using pp collision data collected by the LHCb experiment at centre-of-mass energies of 7, 8, and 13 TeV. The combined data set corresponds to an integrated luminosity of 9 fb^{-1} .

The LHCb detector [14, 15] is a single-arm forward spectrometer covering the pseudorapidity range $2 < \eta < 5$, designed for the study of particles containing b or c quarks. The detector includes a high-precision tracking system consisting of a silicon-strip vertex detector surrounding the pp interaction region [16], a large-area silicon-strip detector located upstream of a dipole magnet with a bending power of about 4 Tm, and three stations of silicon-strip detectors and straw drift tubes [17] placed downstream of the magnet. The tracking system provides a measurement of the momentum, p , of charged particles with a relative uncertainty that varies from 0.5% at low momentum to 1.0% at 200 GeV. The momentum scale of the tracking system is calibrated using samples of $J/\psi \rightarrow \mu^+\mu^-$ and $B^+ \rightarrow J/\psi K^+$ decays collected concurrently with the data sample used for this analysis [18, 19]. The relative accuracy of this procedure is estimated to be 3×10^{-4} using samples of other fully reconstructed b-hadron, K_s^0 , and narrow $\Upsilon(1S)$ resonance decays. Different types of charged hadrons are distinguished using information from two ring-imaging Cherenkov detectors [20]. The online event selection is performed by a trigger [21] which consists of a hardware stage, based on information from the calorimeter and muon systems, followed by a software stage, which applies a full event reconstruction. The software trigger requires a two-, three- or four-track secondary vertex with significant displacement from all primary pp interaction vertices. A multivariate algorithm [22] is used for the identification of secondary vertices consistent with the decay of a b hadron. Simulated data samples are produced using the software packages described in Refs. [23–27].

Samples of Λ_b^0 candidates are formed from $\Lambda_c^+\pi^-$ combinations, where the Λ_c^+ baryon is reconstructed in the $pK^-\pi^+$ final state. All charged final-state particles are required to have particle-identification information consistent with their respective mass hypotheses. Misreconstructed tracks are suppressed by the use of a neural network [28]. To suppress prompt background, the Λ_b^0 decay products are required to have significant χ_{IP}^2 with respect to all PVs in the event, where χ_{IP}^2 of a particle is the difference in χ^2 of the vertex fit of a given PV, when the particle is included or excluded from the fit. The reconstructed Λ_c^+ vertex is required to have a good fit quality and to be significantly displaced from all PVs. The reconstructed Λ_c^+ mass must be within a mass window of ± 25 MeV of the known

¹Natural units with $c = \hbar = 1$ are used throughout this Letter.

value [29]. Pion candidates are combined with Λ_c^+ candidates to form Λ_b^0 candidates, requiring good vertex-fit quality and separation of the Λ_b^0 decay point from any PV in the event. A Boosted Decision Tree (BDT) discriminant [30, 31] is used to further reduce the background level. The BDT exploits fifteen variables, including kinematic variables of the Λ_c^+ and Λ_b^0 candidates, the lifetime of the Λ_b^0 candidate, kinematic variables and quality of particle identification for the final-state pions, kaons and protons, and variables describing the consistency of the selected candidates with the $\Lambda_b^0 \rightarrow \Lambda_c^+ \pi^-$ decay of a Λ_b^0 baryon [32]. The BDT is trained using background-subtracted [33] Λ_b^0 candidates as a signal sample and Λ_b^0 candidates from the data sidebands, in the $\Lambda_c^+ \pi^-$ mass range $5.7 < m_{\Lambda_c^+ \pi^-} < 6.1$ GeV, as a background sample. The k -fold cross-validation technique with $k = 11$ is used in the BDT training [34]. The use of a multivariate discriminant allows the small level of Λ_b^0 background candidates in the analysis to be reduced by a further factor of two, keeping almost 100% efficiency for the signal. The resulting yield of $\Lambda_b^0 \rightarrow \Lambda_c^+ \pi^-$ decays is $(892.8 \pm 1.2) \times 10^3$. A sample of $\Lambda_b^0 \rightarrow J/\psi p K^-$ candidates, with $J/\psi \rightarrow \mu^+ \mu^-$, is also selected in a similar way as a cross-check. The yield for this decay mode is smaller, corresponding to $(217.5 \pm 0.7) \times 10^3$ decays. The mass spectra of the selected $\Lambda_b^0 \rightarrow \Lambda_c^+ \pi^-$ and $\Lambda_b^0 \rightarrow J/\psi p K^-$ candidates are shown in Fig. S1 of the Supplemental Material of this Letter.

The selected Λ_b^0 candidates are combined with pairs of pions compatible with originating from the same PV as the Λ_b^0 candidate. Only pion pairs with $p_T^{\pi^+ \pi^-} > 500$ MeV are used, to suppress the otherwise large combinatorial background from soft dipion combinations. This background is further reduced by using a dedicated BDT discriminant tuned on each of the two samples with $\Lambda_b^0 \rightarrow \Lambda_c^+ \pi^-$ and $\Lambda_b^0 \rightarrow J/\psi p K^-$ decays. It exploits the transverse momentum of the $\Lambda_b^0 \pi^+ \pi^-$ combination, the χ^2 value for the $\Lambda_b^0 \pi^+ \pi^-$ vertex, the transverse momenta of both individual pions and the pion pair, as well as particle-identification and reconstruction-quality [28] variables for both pions. The BDT is trained on simulated samples of excited beauty baryons with a mass of 6.15 GeV as signal and *same-sign* $\Lambda_b^0 \pi^+ \pi^\pm$ combinations in data, with $m_{\Lambda_b^0 \pi^\pm \pi^\pm} < 6.22$ GeV, as background. In simulation unpolarized production of excited beauty baryons is assumed, followed by decays to the $\Lambda_b^0 \pi^+ \pi^-$ final state according to a three-body phase-space decay model.

In order to improve the $\Lambda_b^0 \pi^+ \pi^-$ mass resolution, the $\Lambda_b^0 \pi^+ \pi^-$ combinations are refitted constraining the masses of the Λ_c^+ baryon (or J/ψ meson) to their known values [29] and requiring consistency of the $\Lambda_b^0 \pi^+ \pi^-$ vertex with the PV associated with the Λ_b^0 candidate [32]. The mass of the Λ_b^0 baryon in the fit is constrained to the central value of $m_{\Lambda_b^0} = 5618.62 \pm 0.16 \pm 0.13$ MeV [35], obtained from a combination of the measurements of the Λ_b^0 mass in $\Lambda_b^0 \rightarrow \chi_{c1,2} p K^-$ [35], $\Lambda_b^0 \rightarrow \psi(2S) p K^-$, $\Lambda_b^0 \rightarrow J/\psi \pi^+ \pi^- p K^-$ [36] and $\Lambda_b^0 \rightarrow J/\psi \Lambda$ decay modes [18, 37] by the LHCb collaboration. The mass distributions for selected $\Lambda_b^0 \pi^+ \pi^-$ candidates are shown in Fig. 1. Only Λ_b^0 candidates with a mass within ± 50 (20) MeV (approximately three times the resolution) of the known Λ_b^0 mass for $\Lambda_b^0 \rightarrow \Lambda_c^+ \pi^-$ ($\Lambda_b^0 \rightarrow J/\psi p K^-$) candidates are used. There is a clear excess of $\Lambda_b^0 \pi^+ \pi^-$ candidates around 6.15 GeV over the background for both Λ_b^0 decay modes. The excess is initially treated as originating from a single broad state. The distributions are parameterised by the sum of signal and background components. The signal component is modelled by a relativistic S-wave Breit–Wigner function with Blatt–Weisskopf form factors [38]. The relativistic Breit–Wigner function is convolved with the detector resolution described by the sum of two Gaussian functions with common mean and parameters, which are fixed from simulation. The obtained effective resolution is 1.7 MeV.

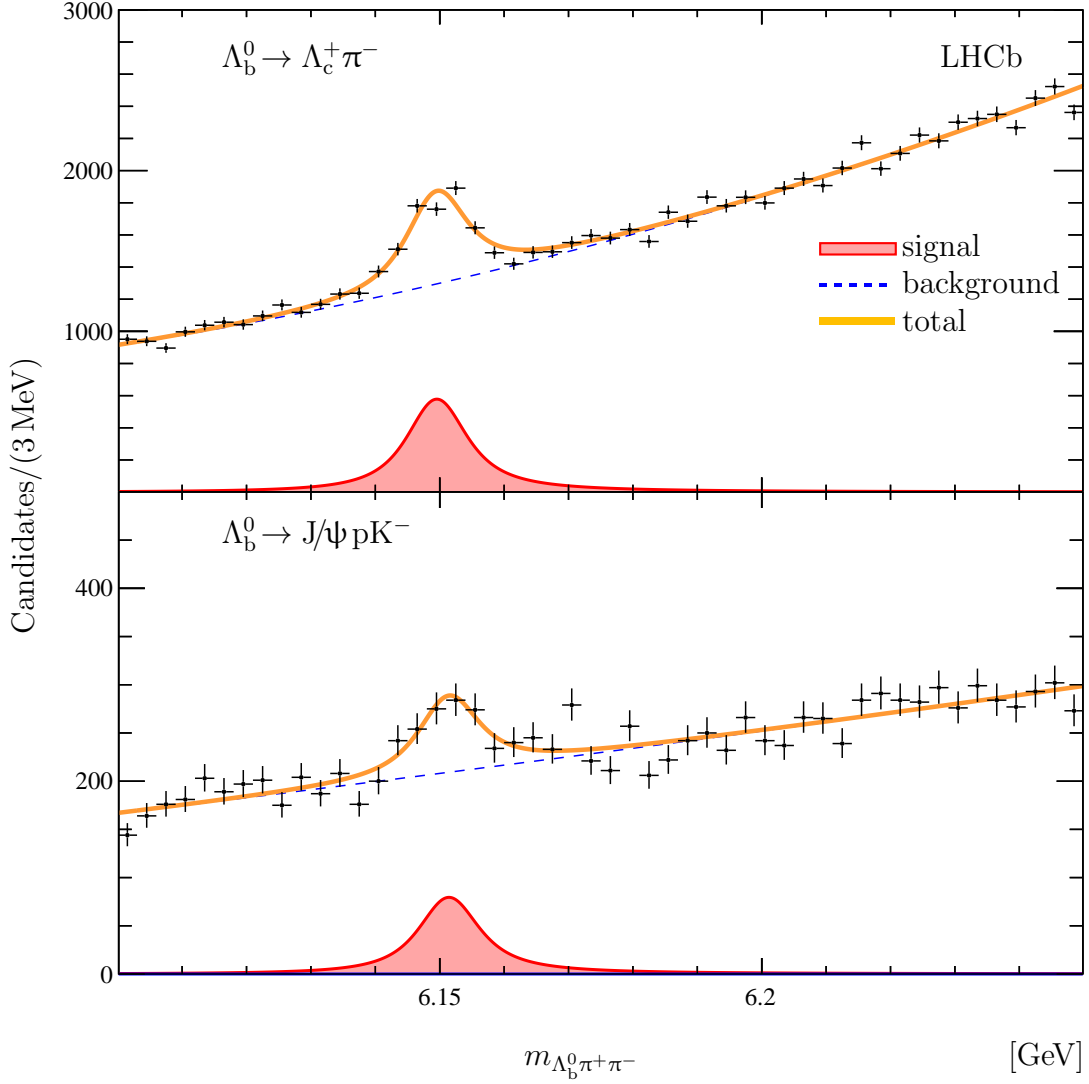


Figure 1: Mass distribution of selected $\Lambda_b^0 \pi^+ \pi^-$ candidates for the (top) $\Lambda_b^0 \rightarrow \Lambda_c^+ \pi^-$ and (bottom) $\Lambda_b^0 \rightarrow J/\psi p K^-$ decay modes.

The background component is parameterised with a second-order polynomial function. Extended unbinned maximum-likelihood fits to the $\Lambda_b^0 \pi^+ \pi^-$ mass spectra are shown in Fig. 1. The corresponding parameters of interest are listed in Table 1.

The mass and width of the structure agree between the $\Lambda_b^0 \rightarrow \Lambda_c^+ \pi^-$ and

Table 1: The yields, N , masses, m , and natural widths, Γ , from the fits of a single broad state to the $\Lambda_b^0 \pi^+ \pi^-$ mass spectra.

		$\Lambda_b^0 \rightarrow \Lambda_c^+ \pi^-$ mode	$\Lambda_b^0 \rightarrow J/\psi p K^-$ mode
$N_{\Lambda_b^0 \pi^+ \pi^-}$		3117 ± 240	431 ± 97
m	[MeV]	6149.6 ± 0.3	6151.5 ± 1.0
Γ	[MeV]	9.6 ± 1.0	9.7 ± 2.9

$\Lambda_b^0 \rightarrow J/\psi p K^-$ samples. The statistical significance for the signals is estimated using Wilks' theorem [39]. It is found to exceed twenty-six and nine standard deviations for the $\Lambda_b^0 \rightarrow \Lambda_c^+ \pi^-$ and $\Lambda_b^0 \rightarrow J/\psi p K^-$ decay modes, respectively. The fitted parameters exhibit very modest dependence on the choice of the orbital momentum for the relativistic Breit–Wigner function and the Blatt–Weiskopf breakup momenta [38]. The signal yields, masses and widths are found to be consistent for the different data-taking periods and between the $\Lambda_b^0 \pi^+ \pi^-$ and $\bar{\Lambda}_b^0 \pi^+ \pi^-$ final states.

Since the mass of the new structure is above the $\Sigma_b^{(*)\pm} \pi^\mp$ kinematic thresholds, the $\Lambda_b^0 \pi^+ \pi^-$ mass spectrum is investigated in $\Lambda_b^0 \pi^\pm$ mass regions populated by the $\Sigma_b^{(*)\pm}$ resonances. The data are split into three nonoverlapping regions: candidates with a $\Lambda_b^0 \pi^\pm$ mass within the natural width of the known Σ_b^\pm mass; candidates with a $\Lambda_b^0 \pi^\pm$ mass within the natural width of the known $\Sigma_b^{*\pm}$ mass; and the remaining nonresonant (NR) region. The $\Lambda_b^0 \pi^+ \pi^-$ mass spectra in these three regions are shown in Fig. 2. Only the larger sample of Λ_b^0 candidates selected via the $\Lambda_b^0 \rightarrow \Lambda_c^+ \pi^-$ decay mode is used here and in the remainder of this Letter. The spectra in the Σ_b and Σ_b^* regions look different and suggest the presence of two narrow peaks.

Doublets of orbitally excited states are predicted in the mass region near the observed peaks [10–13]. The spins and parities of the states in the doublet determine the lowest allowed orbital angular momentum in the two-body $\Sigma_b^{(*)\pm} \pi^\mp$ transition. The intensities of the transitions can be enhanced or suppressed depending on the angular momentum assignment. Heavy quark effective theory (HQET) also predicts different decay rates of the doublet members to the $\Sigma_b^\pm \pi^\mp$ and $\Sigma_b^{*\pm} \pi^\mp$ final states [40]. To probe the two-resonance hypothesis, a simultaneous fit to the mass spectra in the three $\Lambda_b^0 \pi^\pm$ mass regions is performed. For each region, the fit function consists of two signal components and a background component described by a second-order polynomial function. The signal components are modelled by relativistic Breit–Wigner functions convolved with the detector resolution. For the Σ_b region, the signal components describe two-body intermediate states $\Sigma_b^\pm \pi^\mp$ in P- and D-wave for the low-mass and high-mass states, respectively. For the Σ_b^* region, S- and P-wave are chosen for decays of low- and high-mass states, respectively. These choices are motivated by the possible interpretation of the new states as a doublet of $\Lambda_b(1D)^0$ states [10–13]. The masses and widths of the two states are taken as common parameters for the three regions, while the other parameters, namely the signal and background yields and background shape parameters, are allowed to vary independently. The two signal components are added incoherently, assuming interference effects are negligible, since a coherent production of the states in the complex environment of pp interactions is unlikely.

The results of the simultaneous extended unbinned maximum-likelihood fit to the $\Lambda_b^0 \pi^+ \pi^-$ mass spectra in the three $\Lambda_b^0 \pi^\pm$ mass regions are shown in Fig. 2. The two-signal hypothesis is favoured with respect to the single-signal hypothesis with a statistical significance exceeding seven standard deviations. The masses, m , and the natural widths, Γ , of the two narrow states, referred to hereafter as $\Lambda_b(6146)^0$ and $\Lambda_b(6152)^0$,

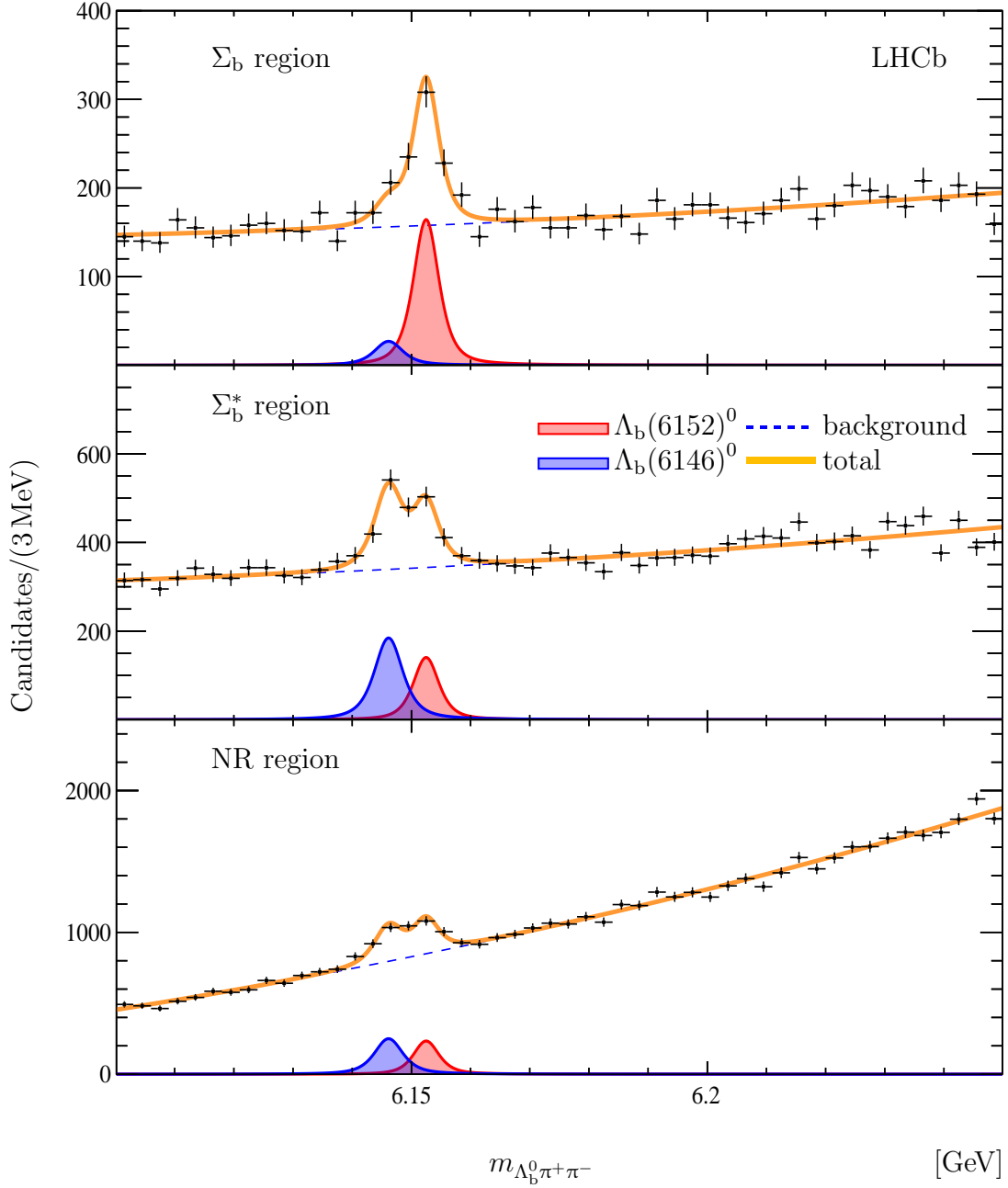


Figure 2: Mass distributions of selected $\Lambda_b^0 \pi^+ \pi^-$ candidates for the three regions in $\Lambda_b^0 \pi^\pm$ mass: (top) Σ_b , (middle) Σ_b^* and (bottom) nonresonant (NR) region.

are measured to be

$$\begin{aligned}
 m_{\Lambda_b(6146)^0} &= 6146.17 \pm 0.33 \text{ MeV} , \\
 m_{\Lambda_b(6152)^0} &= 6152.51 \pm 0.26 \text{ MeV} , \\
 \Gamma_{\Lambda_b(6146)^0} &= 2.9 \pm 1.3 \text{ MeV} , \\
 \Gamma_{\Lambda_b(6152)^0} &= 2.1 \pm 0.8 \text{ MeV} ,
 \end{aligned}$$

with a mass splitting of $\Delta m = 6.34 \pm 0.32 \text{ MeV}$, where the uncertainties are statistical

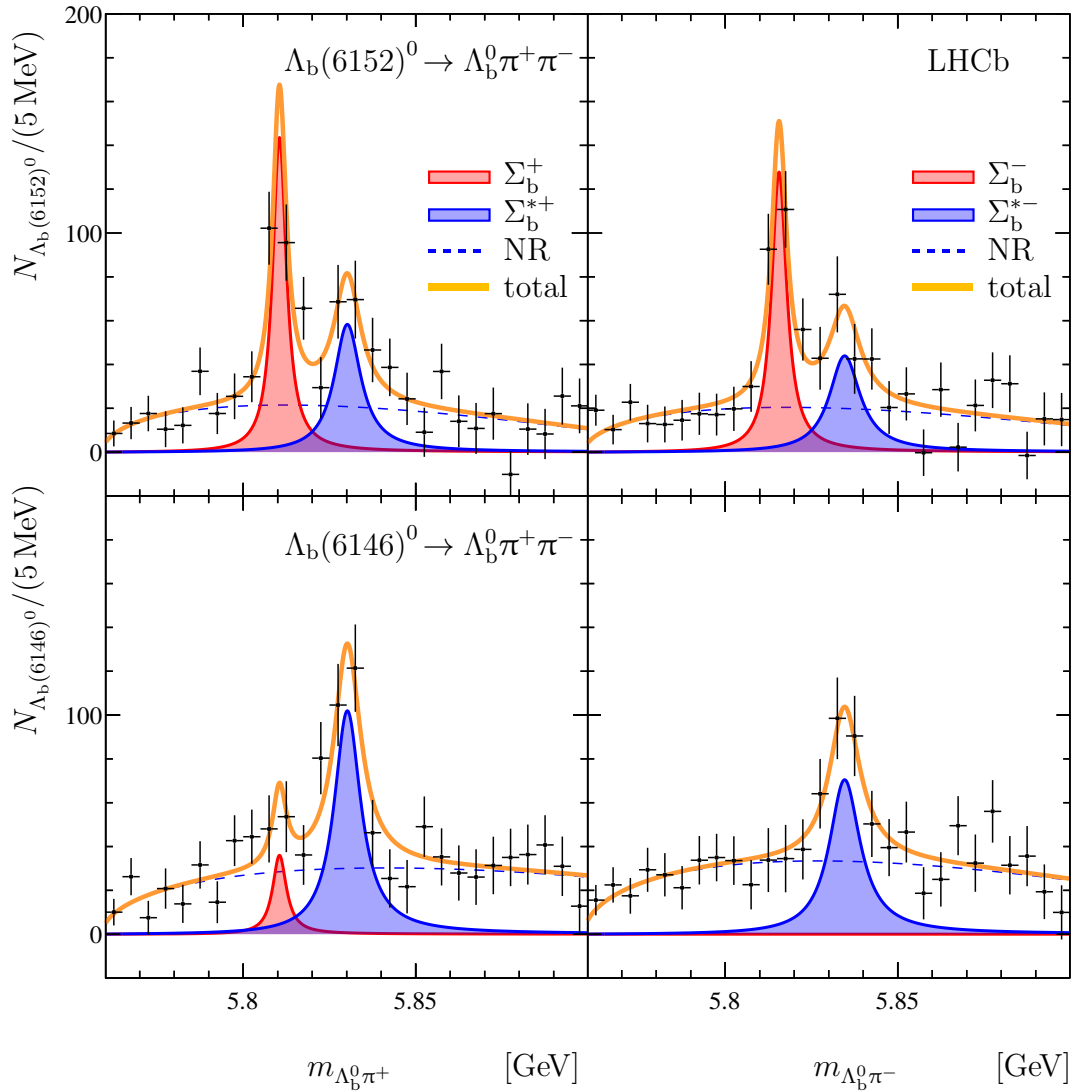


Figure 3: Background-subtracted mass distribution of (left) $\Lambda_b^0\pi^+$ and (right) $\Lambda_b^0\pi^-$ combinations from (top) $\Lambda_b(6152)^0 \rightarrow \Lambda_b^0\pi^+\pi^-$ and (bottom) $\Lambda_b(6146)^0 \rightarrow \Lambda_b^0\pi^+\pi^-$ decays. Results of fits with a model comprising Σ_b , Σ_b^* and nonresonant (NR) components are superimposed.

only. While these new states are denoted as Λ_b , their interpretation as other excited beauty baryons, such as neutral Σ_b^0 states, cannot be excluded.

To probe further the resonance structure of the $\Lambda_b(6146)^0 \rightarrow \Lambda_b^0\pi^+\pi^-$ and $\Lambda_b(6152)^0 \rightarrow \Lambda_b^0\pi^+\pi^-$ decays, the background-subtracted $\Lambda_b^0\pi^\pm$ mass spectra are studied. The SPLIT technique [33] is used here; it projects out the signal components from the combined signal-plus-background densities using $m_{\Lambda_b^0\pi^+\pi^-}$ as a discriminating variable. The resulting $\Lambda_b^0\pi^\pm$ mass spectra are shown in Fig. 3. The spectra are fit with three components, describing the contributions from Σ_b^\pm , $\Sigma_b^{*\pm}$ and nonresonant decays. Relativistic S- and P-wave Breit–Wigner functions are used to describe $\Sigma_b^\pm \rightarrow \Lambda_b^0\pi^\pm$ and $\Sigma_b^{(*)\pm} \rightarrow \Lambda_b^0\pi^\pm$ decays, respectively. The choice of the orbital angular momentum is based on the quark model expectation of spin $\frac{1}{2}$ for Λ_b^0 and Σ_b baryons and $\frac{3}{2}$ for Σ_b^* states. Since the resolution on the $\Lambda_b^0\pi^\pm$ mass is much better than the natural

Table 2: Summary of the systematic uncertainties for the masses, m , and widths, Γ , of the $\Lambda_b(6146)^0$ and $\Lambda_b(6152)^0$ states. All values are in keV.

Source	$\Lambda_b(6146)^0$		$\Lambda_b(6152)^0$	
	m	Γ	m	Γ
Momentum scale	80	—	80	—
Signal model	50	50	50	50
Resolution model	15	270	< 10	310
Background model	30	30	30	20
Total	100	280	100	320
Including Λ_b^0 mass systematic	220	280	220	320

widths of the $\Sigma_b^{(*)\pm}$ states, resolution effects are neglected. The nonresonant component is parameterised as a product of two-from-three-body decay phase space functions [41] and a first-order polynomial function. The masses and widths of the $\Sigma_b^{(*)\pm}$ states are fixed to their known values [8]. The results of extended unbinned maximum-likelihood fits to the background-subtracted $\Lambda_b^0\pi^\pm$ mass distributions are shown in Fig. 3, and are presented in Table S3 of the Supplemental Material. Significant $\Lambda_b(6152)^0 \rightarrow \Sigma_b^\pm\pi^\mp$ and $\Lambda_b(6152)^0 \rightarrow \Sigma_b^{*\pm}\pi^\mp$ signals are observed, accounting for approximately one-third and one-quarter of the signal decays in the sample, respectively. The statistical significance of the contributions is in excess of seven and five standard deviations, respectively. For the $\Lambda_b(6146)^0$ state, $\Lambda_b(6146)^0 \rightarrow \Sigma_b^{*\pm}\pi^\mp$ decays account for about half of the observed decay rate with a statistical significance in excess of six standard deviations. No significant $\Lambda_b(6146)^0 \rightarrow \Sigma_b^\pm\pi^\mp$ signals are observed.

Several sources of systematic uncertainty are considered. The most important source of systematic uncertainty on the mass measurements derives from the knowledge of the momentum scale. This uncertainty is evaluated by varying the momentum scale within its known uncertainty [19] and rerunning the mass fit. The second uncertainty arises from the assumed parameters of the Breit–Wigner functions. To estimate this uncertainty, the orbital angular momentum is changed from $L = 0$ to 2 for all signal components and the Blatt–Weisskopf breakup radii are varied from 1.5 to 5 GeV⁻¹. Since the states are narrow and far from the thresholds, the fitted masses and widths have only very small dependency on the assumed parameters. The maximal changes to the fitted parameters with respect to the baseline fit are assigned as systematic uncertainties. The impact of the background model is evaluated by varying the order of the polynomial functions from two to four. A further source of uncertainty on the determination of the natural widths arises from known differences in resolution between data and simulation. This effect is assessed by varying conservatively the width of the resolution function by $\pm 10\%$, based on previous studies [5, 7, 42–45].

The different sources of systematic uncertainty are summarised in Table 2. In all cases they are smaller than the statistical uncertainties. A large part of the systematic uncertainty cancels for the mass splitting, Δm , between the $\Lambda_b(6146)^0$ and $\Lambda_b(6152)^0$ states. The remaining systematic uncertainty for Δm is 20 keV. An additional uncertainty arises due to the value of the Λ_b^0 mass used in the constrained fit. The statistical uncertainty on the Λ_b^0 mass introduces an uncertainty of 0.16 MeV on the $\Lambda_b(6146)^0$ and $\Lambda_b(6152)^0$ masses. This uncertainty is quoted separately. The systematic uncertainty on the constraint is

correlated, through the momentum scale, with the masses measured in this analysis and is instead included in the final systematic uncertainty in Table 2.

In summary, a new structure with high statistical significance is observed in the $\Lambda_b^0 \pi^+ \pi^-$ mass spectrum using $\Lambda_b^0 \rightarrow \Lambda_c^+ \pi^-$ decays, and confirmed using a sample of Λ_b^0 baryons reconstructed through the $\Lambda_b^0 \rightarrow J/\psi p K^-$ decay. An analysis of the $\Lambda_b^0 \pi^+ \pi^-$ mass spectra for the regions enriched by the $\Sigma_b^{(*)\pm}$ resonances suggests the interpretation of the structure as two almost degenerate narrow states, denoted as $\Lambda_b(6146)^0$ and $\Lambda_b(6152)^0$. The masses and natural widths of these states are measured to be

$$\begin{aligned} m_{\Lambda_b(6146)^0} &= 6146.17 \pm 0.33 \pm 0.22 \pm 0.16 \text{ MeV} , \\ m_{\Lambda_b(6152)^0} &= 6152.51 \pm 0.26 \pm 0.22 \pm 0.16 \text{ MeV} , \\ \Gamma_{\Lambda_b(6146)^0} &= 2.9 \pm 1.3 \pm 0.3 \text{ MeV} , \\ \Gamma_{\Lambda_b(6152)^0} &= 2.1 \pm 0.8 \pm 0.3 \text{ MeV} , \end{aligned}$$

where the first uncertainty is statistical, the second systematic and the third for the mass measurements due to imprecise knowledge of the mass of the Λ_b^0 baryon. The mass differences with respect to the Λ_b^0 mass are measured to be

$$\begin{aligned} m_{\Lambda_b(6146)^0} - m_{\Lambda_b^0} &= 526.55 \pm 0.33 \pm 0.10 \text{ MeV} , \\ m_{\Lambda_b(6152)^0} - m_{\Lambda_b^0} &= 532.89 \pm 0.26 \pm 0.10 \text{ MeV} , \end{aligned}$$

and the mass difference between the two states is measured to be $6.34 \pm 0.32 \pm 0.02$ MeV.

The masses of the two states measured in this analysis are consistent with the predictions for the doublet of $\Lambda_b(1D)^0$ states with quantum numbers (spin J and parity P) $J^P = \frac{3}{2}^+$ and $\frac{5}{2}^+$ [10, 13]. Similar natural widths are expected for the two states of the doublet in HQET [40]. The observed decay pattern, where one of the states decays to both Σ_b with $J^P = \frac{1}{2}^+$ and Σ_b^* with $J^P = \frac{3}{2}^+$, while the other decays primarily to Σ_b^* , is also consistent with the above assignment. However, the interpretation of these states as excited Σ_b^0 states cannot be excluded.

Acknowledgements

We express our gratitude to our colleagues in the CERN accelerator departments for the excellent performance of the LHC. We thank the technical and administrative staff at the LHCb institutes. We acknowledge support from CERN and from the national agencies: CAPES, CNPq, FAPERJ and FINEP (Brazil); MOST and NSFC (China); CNRS/IN2P3 (France); BMBF, DFG and MPG (Germany); INFN (Italy); NWO (Netherlands); MNiSW and NCN (Poland); MEN/IFA (Romania); MSHE (Russia); MinCo (Spain); SNSF and SER (Switzerland); NASU (Ukraine); STFC (United Kingdom); DOE NP and NSF (USA). We acknowledge the computing resources that are provided by CERN, IN2P3 (France), KIT and DESY (Germany), INFN (Italy), SURF (Netherlands), PIC (Spain), GridPP (United Kingdom), RRCKI and Yandex LLC (Russia), CSCS (Switzerland), IFIN-HH (Romania), CBPF (Brazil), PL-GRID (Poland) and OSC (USA). We are indebted to the communities behind the multiple open-source software packages on which we depend. Individual groups or

members have received support from AvH Foundation (Germany); EPLANET, Marie Skłodowska-Curie Actions and ERC (European Union); ANR, Labex P2IO and OCEVU, and Région Auvergne-Rhône-Alpes (France); Key Research Program of Frontier Sciences of CAS, CAS PIFI, and the Thousand Talents Program (China); RFBR, RSF and Yandex LLC (Russia); GVA, XuntaGal and GENCAT (Spain); the Royal Society and the Leverhulme Trust (United Kingdom).

References

- [1] M. Gell-Mann, *A schematic model of baryons and mesons*, Phys. Lett. **8** (1964) 214.
- [2] G. Zweig, *An SU_3 model for strong interaction symmetry and its breaking; Version 1*, Tech. Rep. CERN-TH-401, CERN, Geneva, 1964.
- [3] E. Klempt and J.-M. Richard, *Baryon spectroscopy*, Rev. Mod. Phys. **82** (2010) 1095, arXiv:0901.2055.
- [4] LHCb collaboration, R. Aaij *et al.*, *Observation of excited Λ_b^0 baryons*, Phys. Rev. Lett. **109** (2012) 172003, arXiv:1205.3452.
- [5] LHCb collaboration, R. Aaij *et al.*, *Observation of a new Ξ_b^- resonance*, Phys. Rev. Lett. **121** (2018) 072002, arXiv:1805.09418.
- [6] CMS collaboration, S. Chatrchyan *et al.*, *Observation of a new Ξ_b baryon*, Phys. Rev. Lett. **108** (2012) 252002, arXiv:1204.5955.
- [7] LHCb collaboration, R. Aaij *et al.*, *Observation of two new Ξ_b^- baryon resonances*, Phys. Rev. Lett. **114** (2015) 062004, arXiv:1411.4849.
- [8] LHCb collaboration, R. Aaij *et al.*, *Observation of two resonances in the $\Lambda_b^0\pi^\pm$ systems and precise measurement of Σ_b^\pm and $\Sigma_b^{*\pm}$ properties*, Phys. Rev. Lett. **122** (2019) 012001, arXiv:1809.07752.
- [9] CDF collaboration, T. Aaltonen *et al.*, *Evidence for a bottom baryon resonance Λ_b^{*0} in CDF data*, Phys. Rev. **D88** (2013) 071101, arXiv:1308.1760.
- [10] B. Chen, K.-W. Wei, and A. Zhang, *Investigation of Λ_Q and Ξ_Q baryons in the heavy quark-light diquark picture*, Eur. Phys. J. **A51** (2015) 82, arXiv:1406.6561.
- [11] D. Ebert, R. N. Faustov, and V. O. Galkin, *Spectroscopy and Regge trajectories of heavy baryons in the relativistic quark-diquark picture*, Phys. Rev. **D84** (2011) 014025, arXiv:1105.0583.
- [12] W. Roberts and M. Pervin, *Heavy baryons in a quark model*, Int. J. Mod. Phys. **A23** (2008) 2817, arXiv:0711.2492.
- [13] S. Capstick and N. Isgur, *Baryons in a relativized quark model with chromodynamics*, Phys. Rev. **D34** (1986) 2809.
- [14] LHCb collaboration, A. A. Alves Jr. *et al.*, *The LHCb detector at the LHC*, JINST **3** (2008) S08005.
- [15] LHCb collaboration, R. Aaij *et al.*, *LHCb detector performance*, Int. J. Mod. Phys. **A30** (2015) 1530022, arXiv:1412.6352.
- [16] R. Aaij *et al.*, *Performance of the LHCb Vertex Locator*, JINST **9** (2014) P09007, arXiv:1405.7808.
- [17] R. Arink *et al.*, *Performance of the LHCb Outer Tracker*, JINST **9** (2014) P01002, arXiv:1311.3893.

- [18] LHCb collaboration, R. Aaij *et al.*, *Measurements of the Λ_b^0 , Ξ_b^- , and Ω_b^- baryon masses*, Phys. Rev. Lett. **110** (2013) 182001, [arXiv:1302.1072](#).
- [19] LHCb collaboration, R. Aaij *et al.*, *Precision measurement of D meson mass differences*, JHEP **06** (2013) 065, [arXiv:1304.6865](#).
- [20] M. Adinolfi *et al.*, *Performance of the LHCb RICH detector at the LHC*, Eur. Phys. J. **C73** (2013) 2431, [arXiv:1211.6759](#).
- [21] R. Aaij *et al.*, *The LHCb trigger and its performance in 2011*, JINST **8** (2013) P04022, [arXiv:1211.3055](#).
- [22] V. V. Gligorov and M. Williams, *Efficient, reliable and fast high-level triggering using a bonsai boosted decision tree*, JINST **8** (2013) P02013, [arXiv:1210.6861](#).
- [23] T. Sjöstrand, S. Mrenna, and P. Skands, *PYTHIA 6.4 physics and manual*, JHEP **05** (2006) 026, [arXiv:hep-ph/0603175](#); T. Sjöstrand, S. Mrenna, and P. Skands, *A brief introduction to PYTHIA 8.1*, Comput. Phys. Commun. **178** (2008) 852, [arXiv:0710.3820](#).
- [24] I. Belyaev *et al.*, *Handling of the generation of primary events in GAUSS, the LHCb simulation framework*, J. Phys. Conf. Ser. **331** (2011) 032047.
- [25] D. J. Lange, *The EVTGEN particle decay simulation package*, Nucl. Instrum. Meth. **A462** (2001) 152.
- [26] P. Golonka and Z. Was, *PHOTOS Monte Carlo: A precision tool for QED corrections in Z and W decays*, Eur. Phys. J. **C45** (2006) 97, [arXiv:hep-ph/0506026](#).
- [27] Geant4 collaboration, J. Allison *et al.*, *GEANT4 developments and applications*, IEEE Trans. Nucl. Sci. **53** (2006) 270; Geant4 collaboration, S. Agostinelli *et al.*, *GEANT4: A simulation toolkit*, Nucl. Instrum. Meth. **A506** (2003) 250.
- [28] M. De Cian, S. Farry, P. Seyfert, and S. Stahl, *Fast neural-net based fake track rejection in the LHCb reconstruction*, LHCb-PUB-2017-011, 2017.
- [29] Particle Data Group, M. Tanabashi *et al.*, *Review of particle physics*, Phys. Rev. **D98** (2018) 030001.
- [30] B. P. Roe *et al.*, *Boosted decision trees as an alternative to artificial neural networks for particle identification*, Nucl. Instrum. Meth. **A543** (2005) 577.
- [31] Y. Freund and R. E. Schapire, *A decision-theoretic generalization of on-line learning and an application to boosting*, J. Comput. Syst. Sci. **55** (1997) 119.
- [32] W. D. Hulsbergen, *Decay chain fitting with a Kalman filter*, Nucl. Instrum. Meth. **A552** (2005) 566, [arXiv:physics/0503191](#).
- [33] M. Pivk and F. R. Le Diberder, *sPLOT: A statistical tool to unfold data distributions*, Nucl. Instrum. Meth. **A555** (2005) 356, [arXiv:physics/0402083](#).
- [34] S. Geisser, *Predictive inference: An introduction*, Monographs on statistics and applied probability, Chapman & Hall, New York, 1993.

- [35] LHCb collaboration, R. Aaij *et al.*, *Observation of the decays $\Lambda_b^0 \rightarrow \chi_{c1} p K^-$ and $\Lambda_b^0 \rightarrow \chi_{c2} p K^-$* , Phys. Rev. Lett. **119** (2017) 062001, arXiv:1704.07900.
- [36] LHCb collaboration, R. Aaij *et al.*, *Observation of $\Lambda_b^0 \rightarrow \psi(2S) p K^-$ and $\Lambda_b^0 \rightarrow J/\psi \pi^+ \pi^- p K^-$ decays and a measurement of the Λ_b^0 baryon mass*, JHEP **05** (2016) 132, arXiv:1603.06961.
- [37] LHCb collaboration, R. Aaij *et al.*, *Measurement of b-hadron masses*, Phys. Lett. **B708** (2012) 241, arXiv:1112.4896.
- [38] J. M. Blatt and V. F. Weisskopf, *Theoretical nuclear physics*, Springer, New York, 1952.
- [39] S. S. Wilks, *The large-sample distribution of the likelihood ratio for testing composite hypotheses*, Ann. Math. Stat. **9** (1938) 60.
- [40] N. Isgur and M. B. Wise, *Spectroscopy with heavy quark symmetry*, Phys. Rev. Lett. **66** (1991) 1130.
- [41] E. Byckling and K. Kajantie, *Particle kinematics*, John Wiley and Sons Inc., New York, 1973.
- [42] LHCb collaboration, R. Aaij *et al.*, *Study of beauty hadron decays into pairs of charm hadrons*, Phys. Rev. Lett. **112** (2014) 202001, arXiv:1403.3606.
- [43] LHCb collaboration, R. Aaij *et al.*, *Observation of five new narrow Ω_c^0 states decaying to $\Xi_c^+ K^-$* , Phys. Rev. Lett. **118** (2017) 182001, arXiv:1703.04639.
- [44] LHCb collaboration, R. Aaij *et al.*, *χ_{c1} and χ_{c2} resonance parameters with the decays $\chi_{c1,c2} \rightarrow J/\psi \mu^+ \mu^-$* , Phys. Rev. Lett. **119** (2017) 221801, arXiv:1709.04247.
- [45] LHCb collaboration, R. Aaij *et al.*, *Near-threshold $D\bar{D}$ spectroscopy and observation of a new charmonium state*, JHEP **07** (2019) 035, arXiv:1903.12240.

LHCb collaboration

R. Aaij³⁰, C. Abellán Beteta⁴⁷, T. Ackernley⁵⁷, B. Adeva⁴⁴, M. Adinolfi⁵¹, H. Afsharnia⁸, C.A. Aidala⁷⁸, S. Aiola²⁴, Z. Ajaltouni⁸, S. Akar⁶², P. Albicocco²¹, J. Albrecht¹³, F. Alessio⁴⁵, M. Alexander⁵⁶, A. Alfonso Alberio⁴³, G. Alkhazov³⁶, P. Alvarez Cartelle⁵⁸, A.A. Alves Jr⁴⁴, S. Amato², Y. Amhis¹⁰, L. An²⁰, L. Anderlini²⁰, G. Andreassi⁴⁶, M. Andreotti¹⁹, F. Archilli¹⁵, J. Arnau Romeu⁹, A. Artamonov⁴², M. Artuso⁶⁵, K. Arzymatov⁴⁰, E. Aslanides⁹, M. Atzeni⁴⁷, B. Audurier²⁵, S. Bachmann¹⁵, J.J. Back⁵³, S. Baker⁵⁸, V. Balagura^{10,b}, W. Baldini^{19,45}, A. Baranov⁴⁰, R.J. Barlow⁵⁹, S. Barsuk¹⁰, W. Barter⁵⁸, M. Bartolini²², F. Baryshnikov⁷⁴, G. Bassi²⁷, V. Batozskaya³⁴, B. Batsukh⁶⁵, A. Battig¹³, V. Battista⁴⁶, A. Bay⁴⁶, M. Becker¹³, F. Bedeschi²⁷, I. Bediaga¹, A. Beiter⁶⁵, L.J. Bel³⁰, V. Belavin⁴⁰, S. Belin²⁵, N. Belyi⁴, V. Bellee⁴⁶, K. Belous⁴², I. Belyaev³⁷, G. Bencivenni²¹, E. Ben-Haim¹¹, S. Benson³⁰, S. Beranek¹², A. Berezhnoy³⁸, R. Bernet⁴⁷, D. Berninghoff¹⁵, E. Bertholet¹¹, A. Bertolin²⁶, C. Betancourt⁴⁷, F. Betti^{18,e}, M.O. Bettler⁵², Ia. Bezshyiko⁴⁷, S. Bhasin⁵¹, J. Bhom³², M.S. Bieker¹³, S. Bifani⁵⁰, P. Billoir¹¹, A. Birnkraut¹³, A. Bizzeti^{20,u}, M. Bjørn⁶⁰, M.P. Blago⁴⁵, T. Blake⁵³, F. Blanc⁴⁶, S. Blusk⁶⁵, D. Bobulska⁵⁶, V. Bocci²⁹, O. Boente Garcia⁴⁴, T. Boettcher⁶¹, A. Boldyrev⁷⁵, A. Bondar^{41,x}, N. Bondar³⁶, S. Borghi^{59,45}, M. Borisyak⁴⁰, M. Borsato¹⁵, J.T. Borsuk³², M. Boubdir¹², T.J.V. Bowcock⁵⁷, C. Bozzi^{19,45}, S. Braun¹⁵, A. Brea Rodriguez⁴⁴, M. Brodski⁴⁵, J. Brodzicka³², A. Brossa Gonzalo⁵³, D. Brundu^{25,45}, E. Buchanan⁵¹, A. Buonaura⁴⁷, C. Burr⁴⁵, A. Bursche²⁵, J.S. Butter³⁰, J. Buytaert⁴⁵, W. Byczynski⁴⁵, S. Cadeddu²⁵, H. Cai⁶⁹, R. Calabrese^{19,g}, S. Cali²¹, R. Calladine⁵⁰, M. Calvi^{23,i}, M. Calvo Gomez^{43,m}, A. Camboni^{43,m}, P. Campana²¹, D.H. Campora Perez⁴⁵, L. Capriotti^{18,e}, A. Carbone^{18,e}, G. Carboni²⁸, R. Cardinale²², A. Cardini²⁵, P. Carniti^{23,i}, K. Carvalho Akiba², A. Casais Vidal⁴⁴, G. Casse⁵⁷, M. Cattaneo⁴⁵, G. Cavallero²², R. Cenci^{27,p}, J. Cerasoli⁹, M.G. Chapman⁵¹, M. Charles^{11,45}, Ph. Charpentier⁴⁵, G. Chatzikonstantinidis⁵⁰, M. Chefdeville⁷, V. Chekalina⁴⁰, C. Chen³, S. Chen²⁵, A. Chernov³², S.-G. Chitic⁴⁵, V. Chobanova⁴⁴, M. Chruszcz⁴⁵, A. Chubykin³⁶, P. Ciambone²¹, M.F. Cicala⁵³, X. Cid Vidal⁴⁴, G. Ciezarek⁴⁵, F. Cindolo¹⁸, P.E.L. Clarke⁵⁵, M. Clemencic⁴⁵, H.V. Cliff⁵², J. Closier⁴⁵, J.L. Cobbledick⁵⁹, V. Coco⁴⁵, J.A.B. Coelho¹⁰, J. Cogan⁹, E. Cogneras⁸, L. Cojocariu³⁵, P. Collins⁴⁵, T. Colombo⁴⁵, A. Comerma-Montells¹⁵, A. Contu²⁵, N. Cooke⁵⁰, G. Coombs⁵⁶, S. Coquereau⁴³, G. Corti⁴⁵, C.M. Costa Sobral⁵³, B. Couturier⁴⁵, G.A. Cowan⁵⁵, D.C. Craik⁶¹, A. Crocombe⁵³, M. Cruz Torres¹, R. Currie⁵⁵, C.L. Da Silva⁶⁴, E. Dall'Occo³⁰, J. Dalseno^{44,51}, C. D'Ambrosio⁴⁵, A. Danilina³⁷, P. d'Argent¹⁵, A. Davis⁵⁹, O. De Aguiar Francisco⁴⁵, K. De Bruyn⁴⁵, S. De Capua⁵⁹, M. De Cian⁴⁶, J.M. De Miranda¹, L. De Paula², M. De Serio^{17,d}, P. De Simone²¹, J.A. de Vries³⁰, C.T. Dean⁶⁴, W. Dean⁷⁸, D. Decamp⁷, L. Del Buono¹¹, B. Delaney⁵², H.-P. Dembinski¹⁴, M. Demmer¹³, A. Dendek³³, V. Denysenko⁴⁷, D. Derkach⁷⁵, O. Deschamps⁸, F. Desse¹⁰, F. Dettori²⁵, B. Dey⁶, A. Di Canto⁴⁵, P. Di Nezza²¹, S. Didenko⁷⁴, H. Dijkstra⁴⁵, F. Dordei²⁵, M. Dorigo^{27,y}, A.C. dos Reis¹, A. Dosil Suárez⁴⁴, L. Douglas⁵⁶, A. Dovbnya⁴⁸, K. Dreimanis⁵⁷, M.W. Dudek³², L. Dufour⁴⁵, G. Dujany¹¹, P. Durante⁴⁵, J.M. Durham⁶⁴, D. Dutta⁵⁹, R. Dzhelyadin^{42,†}, M. Dziewiecki¹⁵, A. Dziurda³², A. Dzyuba³⁶, S. Easo⁵⁴, U. Egede⁵⁸, V. Egorychev³⁷, S. Eidelman^{41,x}, S. Eisenhardt⁵⁵, R. Ekelhof¹³, S. Ek-In⁴⁶, L. Eklund⁵⁶, S. Ely⁶⁵, A. Ene³⁵, S. Escher¹², S. Esen³⁰, T. Evans⁴⁵, A. Falabella¹⁸, J. Fan³, N. Farley⁵⁰, S. Farry⁵⁷, D. Fazzini¹⁰, M. Féo⁴⁵, P. Fernandez Declara⁴⁵, A. Fernandez Prieto⁴⁴, F. Ferrari^{18,e}, L. Ferreira Lopes⁴⁶, F. Ferreira Rodrigues², S. Ferreres Sole³⁰, M. Ferro-Luzzi⁴⁵, S. Filippov³⁹, R.A. Fini¹⁷, M. Fiorini^{19,g}, M. Firlej³³, K.M. Fischer⁶⁰, C. Fitzpatrick⁴⁵, T. Fiutowski³³, F. Fleuret^{10,b}, M. Fontana⁴⁵, F. Fontanelli^{22,h}, R. Forty⁴⁵, V. Franco Lima⁵⁷, M. Franco Sevilla⁶³, M. Frank⁴⁵, C. Frei⁴⁵, D.A. Friday⁵⁶, J. Fu^{24,q}, W. Funk⁴⁵, E. Gabriel⁵⁵, A. Gallas Torreira⁴⁴, D. Galli^{18,e}, S. Gallorini²⁶, S. Gambetta⁵⁵, Y. Gan³, M. Gandelman², P. Gandini²⁴, Y. Gao³, L.M. Garcia Martin⁷⁷, J. García Pardiñas⁴⁷, B. Garcia Plana⁴⁴, F.A. Garcia Rosales¹⁰,

J. Garra Tico⁵², L. Garrido⁴³, D. Gascon⁴³, C. Gaspar⁴⁵, G. Gazzoni⁸, D. Gerick¹⁵,
 E. Gersabeck⁵⁹, M. Gersabeck⁵⁹, T. Gershon⁵³, D. Gerstel⁹, Ph. Ghez⁷, V. Gibson⁵²,
 A. Gioventù⁴⁴, O.G. Girard⁴⁶, P. Gironella Gironell⁴³, L. Giubega³⁵, C. Giugliano¹⁹,
 K. Gizdov⁵⁵, V.V. Gligorov¹¹, C. Göbel⁶⁷, D. Golubkov³⁷, A. Golutvin^{58,74}, A. Gomes^{1,a},
 I.V. Gorelov³⁸, C. Gotti^{23,i}, E. Govorkova³⁰, J.P. Grabowski¹⁵, R. Graciani Diaz⁴³,
 T. Grammatico¹¹, L.A. Granado Cardoso⁴⁵, E. Graugés⁴³, E. Graverini⁴⁶, G. Graziani²⁰,
 A. Grecu³⁵, R. Greim³⁰, P. Griffith¹⁹, L. Grillo⁵⁹, L. Gruber⁴⁵, B.R. Gruberg Cazon⁶⁰, C. Gu³,
 E. Gushchin³⁹, A. Guth¹², Yu. Guz^{42,45}, T. Gys⁴⁵, T. Hadavizadeh⁶⁰, C. Hadjivasiliou⁸,
 G. Haefeli⁴⁶, C. Haen⁴⁵, S.C. Haines⁵², P.M. Hamilton⁶³, Q. Han⁶, X. Han¹⁵, T.H. Hancock⁶⁰,
 S. Hansmann-Menzemer¹⁵, N. Harnew⁶⁰, T. Harrison⁵⁷, R. Hart³⁰, C. Hasse⁴⁵, M. Hatch⁴⁵,
 J. He⁴, M. Hecker⁵⁸, K. Heijhoff³⁰, K. Heinicke¹³, A. Heister¹³, A.M. Hennequin⁴⁵,
 K. Hennessy⁵⁷, L. Henry⁷⁷, M. Heß⁷¹, J. Heuel¹², A. Hicheur⁶⁶, R. Hidalgo Charman⁵⁹,
 D. Hill⁶⁰, M. Hilton⁵⁹, P.H. Hopchev⁴⁶, J. Hu¹⁵, W. Hu⁶, W. Huang⁴, Z.C. Huard⁶²,
 W. Hulsbergen³⁰, T. Humair⁵⁸, R.J. Hunter⁵³, M. Hushchyn⁷⁵, D. Hutchcroft⁵⁷, D. Hynds³⁰,
 P. Ibis¹³, M. Idzik³³, P. Ilten⁵⁰, A. Inglese³⁶, A. Inyakin⁴², K. Ivshin³⁶, R. Jacobsson⁴⁵,
 S. Jakobsen⁴⁵, J. Jalocha⁶⁰, E. Jans³⁰, B.K. Jashal⁷⁷, A. Jawahery⁶³, V. Jevtic¹³, F. Jiang³,
 M. John⁶⁰, D. Johnson⁴⁵, C.R. Jones⁵², B. Jost⁴⁵, N. Jurik⁶⁰, S. Kandybei⁴⁸, M. Karacson⁴⁵,
 J.M. Kariuki⁵¹, S. Karodia⁵⁶, N. Kazeev⁷⁵, M. Kecke¹⁵, F. Keizer⁵², M. Kelsey⁶⁵, M. Kenzie⁵²,
 T. Ketel³¹, B. Khanji⁴⁵, A. Kharisova⁷⁶, C. Khurewathanakul⁴⁶, K.E. Kim⁶⁵, T. Kirn¹²,
 V.S. Kirsobom⁴⁶, S. Klaver²¹, K. Klimaszewski³⁴, S. Koliiev⁴⁹, A. Kondybayeva⁷⁴,
 A. Konoplyannikov³⁷, P. Kopciwicz³³, R. Kopečna¹⁵, P. Koppenburg³⁰, I. Kostiuk^{30,49},
 O. Kot⁴⁹, S. Kotriakhova³⁶, M. Kozeiha⁸, L. Kravchuk³⁹, R.D. Krawczyk⁴⁵, M. Kreps⁵³,
 F. Kress⁵⁸, S. Kretzschmar¹², P. Krokovny^{41,x}, W. Krupa³³, W. Krzemien³⁴, W. Kucewicz^{32,l},
 M. Kucharczyk³², V. Kudryavtsev^{41,x}, H.S. Kuindersma³⁰, G.J. Kunde⁶⁴, A.K. Kuonen⁴⁶,
 T. Kvaratskheliya³⁷, D. Lacarrere⁴⁵, G. Lafferty⁵⁹, A. Lai²⁵, D. Lancierini⁴⁷, J.J. Lane⁵⁹,
 G. Lanfranchi²¹, C. Langenbruch¹², T. Latham⁵³, F. Lazzari^{27,v}, C. Lazzeroni⁵⁰, R. Le Gac⁹,
 R. Lefèvre⁸, A. Leflat³⁸, F. Lemaitre⁴⁵, O. Leroy⁹, T. Lesiak³², B. Leverington¹⁵, H. Li⁶⁸,
 P.-R. Li^{4,ab}, X. Li⁶⁴, Y. Li⁵, Z. Li⁶⁵, X. Liang⁶⁵, R. Lindner⁴⁵, F. Lionetto⁴⁷, V. Lisovskyi¹⁰,
 G. Liu⁶⁸, X. Liu³, D. Loh⁵³, A. Loi²⁵, J. Lomba Castro⁴⁴, I. Longstaff⁵⁶, J.H. Lopes²,
 G. Loustau⁴⁷, G.H. Lovell⁵², D. Lucchesi^{26,o}, M. Lucio Martinez³⁰, Y. Luo³, A. Lupato²⁶,
 E. Luppi^{19,g}, O. Lupton⁵³, A. Lusiani²⁷, X. Lyu⁴, S. Maccolini^{18,e}, F. Machefer¹⁰, F. Maciuc³⁵,
 V. Macko⁴⁶, P. Mackowiak¹³, S. Maddrell-Mander⁵¹, L.R. Madhan Mohan⁵¹, O. Maev^{36,45},
 A. Maevskiy⁷⁵, K. Maguire⁵⁹, D. Maisuzenko³⁶, M.W. Majewski³³, S. Malde⁶⁰, B. Malecki⁴⁵,
 A. Malinin⁷³, T. Maltsev^{41,x}, H. Malygina¹⁵, G. Manca^{25,f}, G. Mancinelli⁹,
 R. Manera Escalero⁴³, D. Manuzzi^{18,e}, D. Marangotto^{24,q}, J. Maratas^{8,w}, J.F. Marchand⁷,
 U. Marconi¹⁸, S. Mariani²⁰, C. Marin Benito¹⁰, M. Marinangeli⁴⁶, P. Marino⁴⁶, J. Marks¹⁵,
 P.J. Marshall⁵⁷, G. Martellotti²⁹, L. Martinazzoli⁴⁵, M. Martinelli^{45,23,i}, D. Martinez Santos⁴⁴,
 F. Martinez Vidal⁷⁷, A. Massafferri¹, M. Materok¹², R. Matev⁴⁵, A. Mathad⁴⁷, Z. Mathe⁴⁵,
 V. Matiunin³⁷, C. Matteuzzi²³, K.R. Mattioli⁷⁸, A. Mauri⁴⁷, E. Maurice^{10,b}, M. McCann^{58,45},
 L. McConnell¹⁶, A. McNab⁵⁹, R. McNulty¹⁶, J.V. Mead⁵⁷, B. Meadows⁶², C. Meaux⁹,
 N. Meinert⁷¹, D. Melnychuk³⁴, S. Meloni^{23,i}, M. Merk³⁰, A. Merli^{24,q}, E. Michielin²⁶,
 D.A. Milanese⁷⁰, E. Millard⁵³, M.-N. Minard⁷, O. Mineev³⁷, L. Minzoni^{19,g}, S.E. Mitchell⁵⁵,
 B. Mitreska⁵⁹, D.S. Mitzel⁴⁵, A. Mödden¹³, A. Mogini¹¹, R.D. Moise⁵⁸, T. Mombächer¹³,
 I.A. Monroy⁷⁰, S. Monteil⁸, M. Morandin²⁶, G. Morello²¹, M.J. Morello^{27,t}, J. Moron³³,
 A.B. Morris⁹, A.G. Morris⁵³, R. Mountain⁶⁵, H. Mu³, F. Muheim⁵⁵, M. Mukherjee⁶,
 M. Mulder³⁰, D. Müller⁴⁵, J. Müller¹³, K. Müller⁴⁷, V. Müller¹³, C.H. Murphy⁶⁰, D. Murray⁵⁹,
 P. Muzzetto²⁵, P. Naik⁵¹, T. Nakada⁴⁶, R. Nandakumar⁵⁴, A. Nandi⁶⁰, T. Namut⁴⁶, I. Nasteva²,
 M. Needham⁵⁵, N. Neri^{24,q}, S. Neubert¹⁵, N. Neufeld⁴⁵, R. Newcombe⁵⁸, T.D. Nguyen⁴⁶,
 C. Nguyen-Mau^{46,n}, E.M. Niel¹⁰, S. Nieswand¹², N. Nikitin³⁸, N.S. Nolte⁴⁵,
 A. Oblakowska-Mucha³³, V. Obraztsov⁴², S. Ogilvy⁵⁶, D.P. O'Hanlon¹⁸, R. Oldeman^{25,f},

C.J.G. Onderwater⁷², J. D. Osborn⁷⁸, A. Ossowska³², J.M. Otalora Goicochea²,
 T. Ovsiannikova³⁷, P. Owen⁴⁷, A. Oyanguren⁷⁷, P.R. Pais⁴⁶, T. Pajero^{27,t}, A. Palano¹⁷,
 M. Palutan²¹, G. Panshin⁷⁶, A. Papanestis⁵⁴, M. Pappagallo⁵⁵, L.L. Pappalardo^{19,g},
 W. Parker⁶³, C. Parkes^{59,45}, G. Passaleva^{20,45}, A. Pastore¹⁷, M. Patel⁵⁸, C. Patrignani^{18,e},
 A. Pearce⁴⁵, A. Pellegrino³⁰, G. Penso²⁹, M. Pepe Altarelli⁴⁵, S. Perazzini¹⁸, D. Pereima³⁷,
 P. Perret⁸, L. Pescatore⁴⁶, K. Petridis⁵¹, A. Petrolini^{22,h}, A. Petrov⁷³, S. Petrucci⁵⁵,
 M. Petruzzo^{24,q}, B. Pietrzyk⁷, G. Pietrzyk⁴⁶, M. Pikies³², M. Pili⁶⁰, D. Pinci²⁹, J. Pinzino⁴⁵,
 F. Pisani⁴⁵, A. Piucci¹⁵, V. Placinta³⁵, S. Playfer⁵⁵, J. Plews⁵⁰, M. Plo Casasus⁴⁴, F. Polci¹¹,
 M. Poli Lener²¹, M. Poliakov⁶⁵, A. Poluektov⁹, N. Polukhina^{74,c}, I. Polyakov⁶⁵, E. Polcarpo²,
 G.J. Pomery⁵¹, S. Ponce⁴⁵, A. Popov⁴², D. Popov⁵⁰, S. Poslavskii⁴², K. Prasanth³²,
 L. Promberger⁴⁵, C. Prouve⁴⁴, V. Pugatch⁴⁹, A. Puig Navarro⁴⁷, H. Pullen⁶⁰, G. Punzi^{27,p},
 W. Qian⁴, J. Qin⁴, R. Quagliani¹¹, B. Quintana⁸, N.V. Raab¹⁶, B. Rachwal³³,
 J.H. Rademacker⁵¹, M. Rama²⁷, M. Ramos Pernas⁴⁴, M.S. Rangel², F. Ratnikov^{40,75},
 G. Raven³¹, M. Ravonel Salzgeber⁴⁵, M. Reboud⁷, F. Redi⁴⁶, S. Reichert¹³, F. Reiss¹¹,
 C. Remon Alepuz⁷⁷, Z. Ren³, V. Renaudin⁶⁰, S. Ricciardi⁵⁴, S. Richards⁵¹, K. Rinnert⁵⁷,
 P. Robbe¹⁰, A. Robert¹¹, A.B. Rodrigues⁴⁶, E. Rodrigues⁶², J.A. Rodriguez Lopez⁷⁰,
 M. Roehrken⁴⁵, S. Roiser⁴⁵, A. Rollings⁶⁰, V. Romanovskiy⁴², M. Romero Lamas⁴⁴,
 A. Romero Vidal⁴⁴, J.D. Roth⁷⁸, M. Rotondo²¹, M.S. Rudolph⁶⁵, T. Ruf⁴⁵, J. Ruiz Vidal⁷⁷,
 J. Ryzka³³, J.J. Saborido Silva⁴⁴, N. Sagidova³⁶, B. Saitta^{25,f}, C. Sanchez Gras³⁰,
 C. Sanchez Mayordomo⁷⁷, B. Sanmartin Sedes⁴⁴, R. Santacesaria²⁹, C. Santamarina Rios⁴⁴,
 P. Santangelo²¹, M. Santimaria^{21,45}, E. Santovetti^{28,j}, G. Sarpis⁵⁹, A. Sarti²⁹, C. Satriano^{29,s},
 A. Satta²⁸, M. Saur⁴, D. Savrina^{37,38}, L.G. Scantlebury Smead⁶⁰, S. Schael¹², M. Schellenberg¹³,
 M. Schiller⁵⁶, H. Schindler⁴⁵, M. Schmelling¹⁴, T. Schmelzer¹³, B. Schmidt⁴⁵, O. Schneider⁴⁶,
 A. Schopper⁴⁵, H.F. Schreiner⁶², M. Schubiger³⁰, S. Schulte⁴⁶, M.H. Schune¹⁰, R. Schwemmer⁴⁵,
 B. Sciascia²¹, A. Sciubba^{29,k}, S. Sellam⁶⁶, A. Semennikov³⁷, A. Sergi^{50,45}, N. Serra⁴⁷,
 J. Serrano⁹, L. Sestini²⁶, A. Seuthe¹³, P. Seyfert⁴⁵, D.M. Shangase⁷⁸, M. Shapkin⁴², T. Shears⁵⁷,
 L. Shekhtman^{41,x}, V. Shevchenko^{73,74}, E. Shmanin⁷⁴, J.D. Shupperd⁶⁵, B.G. Siddi¹⁹,
 R. Silva Coutinho⁴⁷, L. Silva de Oliveira², G. Simi^{26,o}, S. Simone^{17,d}, I. Skiba¹⁹, N. Skidmore¹⁵,
 T. Skwarnicki⁶⁵, M.W. Slater⁵⁰, J.G. Smeaton⁵², E. Smith¹², I.T. Smith⁵⁵, M. Smith⁵⁸,
 M. Soares¹⁸, I. Soares Lavra¹, M.D. Sokoloff⁶², F.J.P. Soler⁵⁶, B. Souza De Paula², B. Spaan¹³,
 E. Spadaro Norella^{24,q}, P. Spradlin⁵⁶, F. Stagni⁴⁵, M. Stahl⁶², S. Stahl⁴⁵, P. Stefko⁴⁶,
 S. Stefkova⁵⁸, O. Steinkamp⁴⁷, S. Stemmler¹⁵, O. Stenyakin⁴², M. Stepanova³⁶, H. Stevens¹³,
 A. Stocchi¹⁰, S. Stone⁶⁵, S. Stracka²⁷, M.E. Stramaglia⁴⁶, M. Straticiu³⁵, U. Straumann⁴⁷,
 S. Strokov⁷⁶, J. Sun³, L. Sun⁶⁹, Y. Sun⁶³, P. Svihra⁵⁹, K. Swientek³³, A. Szabelski³⁴,
 T. Szumlak³³, M. Szymanski⁴, S. Taneja⁵⁹, Z. Tang³, T. Tekampe¹³, G. Tellarini¹⁹,
 F. Teubert⁴⁵, E. Thomas⁴⁵, K.A. Thomson⁵⁷, M.J. Tilley⁵⁸, V. Tisserand⁸, S. T'Jampens⁷,
 M. Tobin⁵, S. Tolk⁴⁵, L. Tomassetti^{19,g}, D. Tonelli²⁷, D.Y. Tou¹¹, E. Tournefier⁷, M. Traill⁵⁶,
 M.T. Tran⁴⁶, A. Trisovic⁵², A. Tsaregorodtsev⁹, G. Tuci^{27,45,p}, A. Tully⁵², N. Tuning³⁰,
 A. Ukleja³⁴, A. Usachov¹⁰, A. Ustyuzhanin^{40,75}, U. Uwer¹⁵, A. Vagner⁷⁶, V. Vagnoni¹⁸,
 A. Valassi⁴⁵, S. Valat⁴⁵, G. Valenti¹⁸, M. van Beuzekom³⁰, H. Van Hecke⁶⁴, E. van Herwijnen⁴⁵,
 C.B. Van Hulse¹⁶, J. van Tilburg³⁰, M. van Veghel⁷², R. Vazquez Gomez⁴⁵,
 P. Vazquez Regueiro⁴⁴, C. Vázquez Sierra³⁰, S. Vecchi¹⁹, J.J. Velthuis⁵¹, M. Veltri^{20,r},
 A. Venkateswaran⁶⁵, M. Vernet⁸, M. Veronesi³⁰, M. Vesterinen⁵³, J.V. Viana Barbosa⁴⁵,
 D. Vieira⁴, M. Vieites Diaz⁴⁶, H. Viemann⁷¹, X. Vilasis-Cardona^{43,m}, A. Vitkovskiy³⁰,
 V. Volkov³⁸, A. Vollhardt⁴⁷, D. Vom Bruch¹¹, B. Voneki⁴⁵, A. Vorobyev³⁶, V. Vorobyev^{41,x},
 N. Voropaev³⁶, R. Waldi⁷¹, J. Walsh²⁷, J. Wang³, J. Wang⁵, M. Wang³, Y. Wang⁶, Z. Wang⁴⁷,
 D.R. Ward⁵², H.M. Wark⁵⁷, N.K. Watson⁵⁰, D. Websdale⁵⁸, A. Weiden⁴⁷, C. Weisser⁶¹,
 B.D.C. Westhenry⁵¹, D.J. White⁵⁹, M. Whitehead¹², D. Wiedner¹³, G. Wilkinson⁶⁰,
 M. Wilkinson⁶⁵, I. Williams⁵², M. Williams⁶¹, M.R.J. Williams⁵⁹, T. Williams⁵⁰, F.F. Wilson⁵⁴,
 M. Winn¹⁰, W. Wislicki³⁴, M. Witek³², G. Wormser¹⁰, S.A. Wotton⁵², H. Wu⁶⁵, K. Wyllie⁴⁵,

Z. Xiang⁴, D. Xiao⁶, Y. Xie⁶, H. Xing⁶⁸, A. Xu³, L. Xu³, M. Xu⁶, Q. Xu⁴, Z. Xu⁷, Z. Xu³,
 Z. Yang³, Z. Yang⁶³, Y. Yao⁶⁵, L.E. Yeomans⁵⁷, H. Yin⁶, J. Yu^{6,aa}, X. Yuan⁶⁵,
 O. Yushchenko⁴², K.A. Zarebski⁵⁰, M. Zavertyaev^{14,c}, M. Zdybal³², M. Zeng³, D. Zhang⁶,
 L. Zhang³, S. Zhang³, W.C. Zhang^{3,z}, Y. Zhang⁴⁵, A. Zhelezov¹⁵, Y. Zheng⁴, X. Zhou⁴,
 Y. Zhou⁴, X. Zhu³, V. Zhukov^{12,38}, J.B. Zonneveld⁵⁵, S. Zucchelli^{18,e}.

¹*Centro Brasileiro de Pesquisas Físicas (CBPF), Rio de Janeiro, Brazil*

²*Universidade Federal do Rio de Janeiro (UFRJ), Rio de Janeiro, Brazil*

³*Center for High Energy Physics, Tsinghua University, Beijing, China*

⁴*University of Chinese Academy of Sciences, Beijing, China*

⁵*Institute Of High Energy Physics (ihep), Beijing, China*

⁶*Institute of Particle Physics, Central China Normal University, Wuhan, Hubei, China*

⁷*Univ. Grenoble Alpes, Univ. Savoie Mont Blanc, CNRS, IN2P3-LAPP, Annecy, France*

⁸*Université Clermont Auvergne, CNRS/IN2P3, LPC, Clermont-Ferrand, France*

⁹*Aix Marseille Univ, CNRS/IN2P3, CPPM, Marseille, France*

¹⁰*LAL, Univ. Paris-Sud, CNRS/IN2P3, Université Paris-Saclay, Orsay, France*

¹¹*LPNHE, Sorbonne Université, Paris Diderot Sorbonne Paris Cité, CNRS/IN2P3, Paris, France*

¹²*I. Physikalisches Institut, RWTH Aachen University, Aachen, Germany*

¹³*Fakultät Physik, Technische Universität Dortmund, Dortmund, Germany*

¹⁴*Max-Planck-Institut für Kernphysik (MPIK), Heidelberg, Germany*

¹⁵*Physikalisches Institut, Ruprecht-Karls-Universität Heidelberg, Heidelberg, Germany*

¹⁶*School of Physics, University College Dublin, Dublin, Ireland*

¹⁷*INFN Sezione di Bari, Bari, Italy*

¹⁸*INFN Sezione di Bologna, Bologna, Italy*

¹⁹*INFN Sezione di Ferrara, Ferrara, Italy*

²⁰*INFN Sezione di Firenze, Firenze, Italy*

²¹*INFN Laboratori Nazionali di Frascati, Frascati, Italy*

²²*INFN Sezione di Genova, Genova, Italy*

²³*INFN Sezione di Milano-Bicocca, Milano, Italy*

²⁴*INFN Sezione di Milano, Milano, Italy*

²⁵*INFN Sezione di Cagliari, Monserrato, Italy*

²⁶*INFN Sezione di Padova, Padova, Italy*

²⁷*INFN Sezione di Pisa, Pisa, Italy*

²⁸*INFN Sezione di Roma Tor Vergata, Roma, Italy*

²⁹*INFN Sezione di Roma La Sapienza, Roma, Italy*

³⁰*Nikhef National Institute for Subatomic Physics, Amsterdam, Netherlands*

³¹*Nikhef National Institute for Subatomic Physics and VU University Amsterdam, Amsterdam, Netherlands*

³²*Henryk Niewodniczanski Institute of Nuclear Physics Polish Academy of Sciences, Kraków, Poland*

³³*AGH - University of Science and Technology, Faculty of Physics and Applied Computer Science, Kraków, Poland*

³⁴*National Center for Nuclear Research (NCBJ), Warsaw, Poland*

³⁵*Horia Hulubei National Institute of Physics and Nuclear Engineering, Bucharest-Magurele, Romania*

³⁶*Petersburg Nuclear Physics Institute NRC Kurchatov Institute (PNPI NRC KI), Gatchina, Russia*

³⁷*Institute of Theoretical and Experimental Physics NRC Kurchatov Institute (ITEP NRC KI), Moscow, Russia, Moscow, Russia*

³⁸*Institute of Nuclear Physics, Moscow State University (SINP MSU), Moscow, Russia*

³⁹*Institute for Nuclear Research of the Russian Academy of Sciences (INR RAS), Moscow, Russia*

⁴⁰*Yandex School of Data Analysis, Moscow, Russia*

⁴¹*Budker Institute of Nuclear Physics (SB RAS), Novosibirsk, Russia*

⁴²*Institute for High Energy Physics NRC Kurchatov Institute (IHEP NRC KI), Protvino, Russia, Protvino, Russia*

⁴³*ICCUB, Universitat de Barcelona, Barcelona, Spain*

⁴⁴*Instituto Galego de Física de Altas Enerxías (IGFAE), Universidade de Santiago de Compostela, Santiago de Compostela, Spain*

⁴⁵*European Organization for Nuclear Research (CERN), Geneva, Switzerland*

- ⁴⁶*Institute of Physics, Ecole Polytechnique Fédérale de Lausanne (EPFL), Lausanne, Switzerland*
- ⁴⁷*Physik-Institut, Universität Zürich, Zürich, Switzerland*
- ⁴⁸*NSC Kharkiv Institute of Physics and Technology (NSC KIPT), Kharkiv, Ukraine*
- ⁴⁹*Institute for Nuclear Research of the National Academy of Sciences (KINR), Kyiv, Ukraine*
- ⁵⁰*University of Birmingham, Birmingham, United Kingdom*
- ⁵¹*H.H. Wills Physics Laboratory, University of Bristol, Bristol, United Kingdom*
- ⁵²*Cavendish Laboratory, University of Cambridge, Cambridge, United Kingdom*
- ⁵³*Department of Physics, University of Warwick, Coventry, United Kingdom*
- ⁵⁴*STFC Rutherford Appleton Laboratory, Didcot, United Kingdom*
- ⁵⁵*School of Physics and Astronomy, University of Edinburgh, Edinburgh, United Kingdom*
- ⁵⁶*School of Physics and Astronomy, University of Glasgow, Glasgow, United Kingdom*
- ⁵⁷*Oliver Lodge Laboratory, University of Liverpool, Liverpool, United Kingdom*
- ⁵⁸*Imperial College London, London, United Kingdom*
- ⁵⁹*School of Physics and Astronomy, University of Manchester, Manchester, United Kingdom*
- ⁶⁰*Department of Physics, University of Oxford, Oxford, United Kingdom*
- ⁶¹*Massachusetts Institute of Technology, Cambridge, MA, United States*
- ⁶²*University of Cincinnati, Cincinnati, OH, United States*
- ⁶³*University of Maryland, College Park, MD, United States*
- ⁶⁴*Los Alamos National Laboratory (LANL), Los Alamos, United States*
- ⁶⁵*Syracuse University, Syracuse, NY, United States*
- ⁶⁶*Laboratory of Mathematical and Subatomic Physics , Constantine, Algeria, associated to ²*
- ⁶⁷*Pontifícia Universidade Católica do Rio de Janeiro (PUC-Rio), Rio de Janeiro, Brazil, associated to ²*
- ⁶⁸*South China Normal University, Guangzhou, China, associated to ³*
- ⁶⁹*School of Physics and Technology, Wuhan University, Wuhan, China, associated to ³*
- ⁷⁰*Departamento de Física , Universidad Nacional de Colombia, Bogota, Colombia, associated to ¹¹*
- ⁷¹*Institut für Physik, Universität Rostock, Rostock, Germany, associated to ¹⁵*
- ⁷²*Van Swinderen Institute, University of Groningen, Groningen, Netherlands, associated to ³⁰*
- ⁷³*National Research Centre Kurchatov Institute, Moscow, Russia, associated to ³⁷*
- ⁷⁴*National University of Science and Technology “MISIS”, Moscow, Russia, associated to ³⁷*
- ⁷⁵*National Research University Higher School of Economics, Moscow, Russia, associated to ⁴⁰*
- ⁷⁶*National Research Tomsk Polytechnic University, Tomsk, Russia, associated to ³⁷*
- ⁷⁷*Instituto de Física Corpuscular, Centro Mixto Universidad de Valencia - CSIC, Valencia, Spain, associated to ⁴³*
- ⁷⁸*University of Michigan, Ann Arbor, United States, associated to ⁶⁵*

^a*Universidade Federal do Triângulo Mineiro (UFTM), Uberaba-MG, Brazil*

^b*Laboratoire Leprince-Ringuet, Palaiseau, France*

^c*P.N. Lebedev Physical Institute, Russian Academy of Science (LPI RAS), Moscow, Russia*

^d*Università di Bari, Bari, Italy*

^e*Università di Bologna, Bologna, Italy*

^f*Università di Cagliari, Cagliari, Italy*

^g*Università di Ferrara, Ferrara, Italy*

^h*Università di Genova, Genova, Italy*

ⁱ*Università di Milano Bicocca, Milano, Italy*

^j*Università di Roma Tor Vergata, Roma, Italy*

^k*Università di Roma La Sapienza, Roma, Italy*

^l*AGH - University of Science and Technology, Faculty of Computer Science, Electronics and Telecommunications, Kraków, Poland*

^m*LIFAELS, La Salle, Universitat Ramon Llull, Barcelona, Spain*

ⁿ*Hanoi University of Science, Hanoi, Vietnam*

^o*Università di Padova, Padova, Italy*

^p*Università di Pisa, Pisa, Italy*

^q*Università degli Studi di Milano, Milano, Italy*

^r*Università di Urbino, Urbino, Italy*

^s*Università della Basilicata, Potenza, Italy*

^t*Scuola Normale Superiore, Pisa, Italy*

^u*Università di Modena e Reggio Emilia, Modena, Italy*

^v *Università di Siena, Siena, Italy*

^w *MSU - Iligan Institute of Technology (MSU-IIT), Iligan, Philippines*

^x *Novosibirsk State University, Novosibirsk, Russia*

^y *Sezione INFN di Trieste, Trieste, Italy*

^z *School of Physics and Information Technology, Shaanxi Normal University (SNNU), Xi'an, China*

^{aa} *Physics and Micro Electronic College, Hunan University, Changsha City, China*

^{ab} *Lanzhou University, Lanzhou, China*

[†] *Deceased*

Observation of new resonances in the $\Lambda_b^0 \pi^+ \pi^-$ system

Supplemental Material

The $\Lambda_b^0 \rightarrow \Lambda_c^+ \pi^-$ and $\Lambda_b^0 \rightarrow J/\psi p K^-$ candidates

The mass distributions for selected $\Lambda_b^0 \rightarrow \Lambda_c^+ \pi^-$ and $\Lambda_b^0 \rightarrow J/\psi p K^-$ candidates are shown in Fig. S1. The distributions are fit with a sum of a signal and a background component. The signal component is parameterised by a modified Gaussian function with power-law tails on both sides of the peak,

$$G(m; \mu, \sigma, \alpha_L, \alpha_R, n_L, n_R) \propto \begin{cases} A_L \left(\frac{n_L+1}{n_L+1-\alpha_L(\alpha_L+\delta m)} \right)^{n_L+1} & \text{for } \delta m < -\alpha_L, \\ \frac{1}{\sqrt{2\pi}\sigma} e^{-\frac{1}{2}\delta m^2} & \text{for } -\alpha_L < \delta m < \alpha_R, \\ A_R \left(\frac{n_R+1}{n_R+1-\alpha_R(\alpha_R-\delta m)} \right)^{n_R+1} & \text{for } \delta m > \alpha_R, \end{cases}$$

where $\delta m \equiv \frac{m-\mu}{\sigma}$, $n_{L,R} > 0$, $\alpha_{L,R} > 0$ and $A_{L,R} = \frac{1}{\sqrt{2\pi}\sigma} e^{-\frac{1}{2}\alpha_{L,R}^2}$. The background is parameterised by the product of an exponential function and a second-order polynomial function. The signal yields are listed in Table S1.

Table S1: The signal yields for $\Lambda_b^0 \rightarrow \Lambda_c^+ \pi^-$ and $\Lambda_b^0 \rightarrow J/\psi p K^-$ decays.

Decay mode	N [10^3]
$\Lambda_b^0 \rightarrow \Lambda_c^+ \pi^-$	892.8 ± 1.2
$\Lambda_b^0 \rightarrow J/\psi p K^-$	217.5 ± 0.7

Results of the simultaneous fit to $\Lambda_b^0 \pi^+ \pi^-$ mass spectra in the three $\Lambda_b^0 \pi^\pm$ mass regions

The yields of the $\Lambda_b(6146)^0$ and $\Lambda_b(6152)^0$ signals from the simultaneous extended unbinned maximum-likelihood fit to the $\Lambda_b^0 \pi^+ \pi^-$ mass spectra in the three $\Lambda_b^0 \pi^\pm$ mass regions are presented in Table. S2.

Table S2: The yields of the $\Lambda_b(6146)^0$ and $\Lambda_b(6152)^0$ signals in the three $\Lambda_b^0 \pi^\pm$ mass regions.

	Σ_b region	Σ_b^* region	NR region
$N_{\Lambda_b(6146)^0}$	67 ± 40	460 ± 92	624 ± 136
$N_{\Lambda_b(6152)^0}$	357 ± 52	305 ± 70	510 ± 109

Results of the fits to background-subtracted $\Lambda_b^0 \pi^\pm$ mass spectra

The yield of $\Lambda_b(6146)^0 \rightarrow \Sigma_b^{(*)\pm} \pi^\mp$ and $\Lambda_b(6152)^0 \rightarrow \Sigma_b^{(*)\pm} \pi^\mp$ decays, determined from fits to the background-subtracted $\Lambda_b^0 \pi^\pm$ mass distributions, are summarized in Table S3.

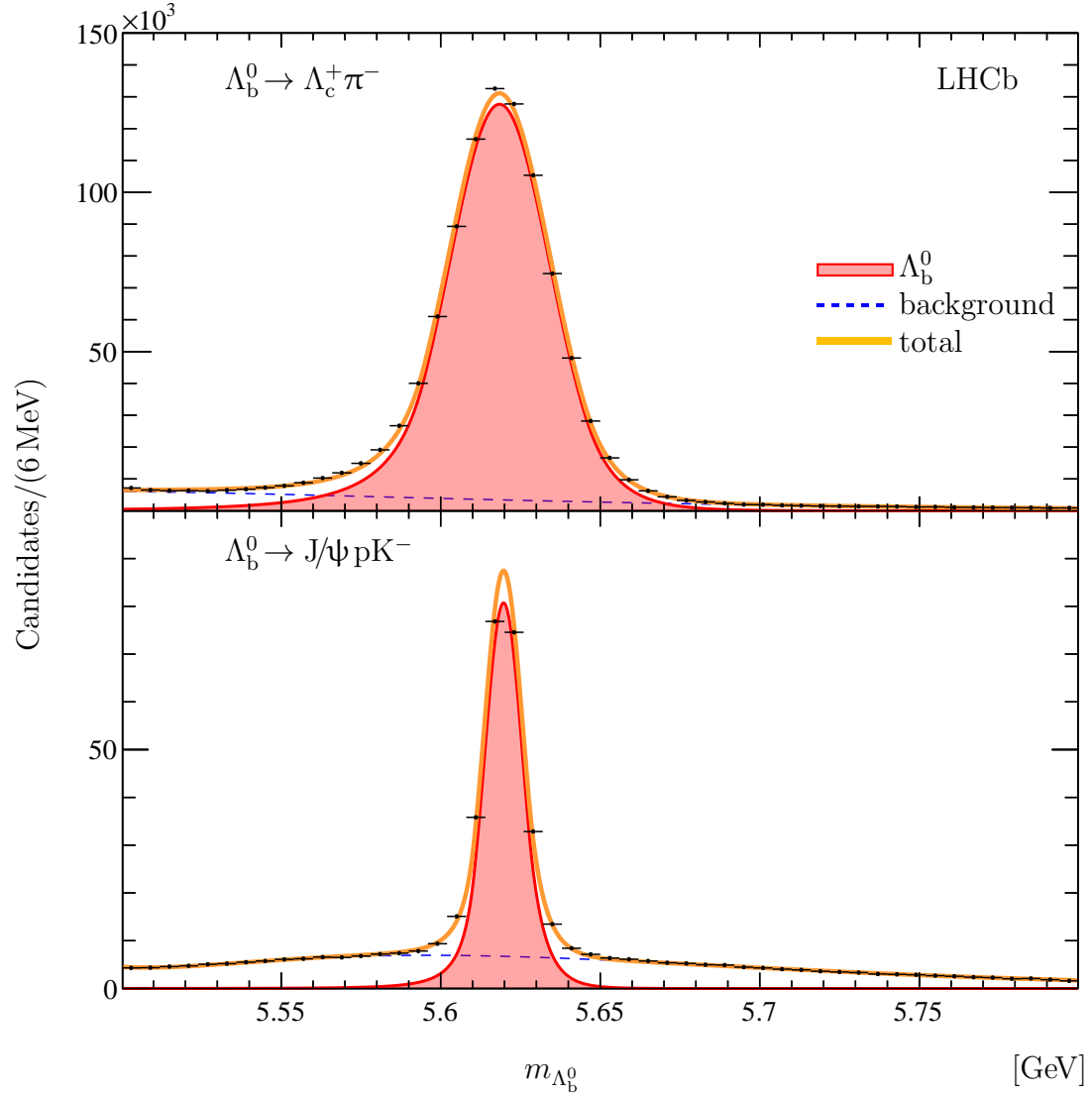


Figure S1: Mass distribution of selected Λ_b^0 candidates from the (top) $\Lambda_b^0 \rightarrow \Lambda_c^+ \pi^-$ and (bottom) $\Lambda_b^0 \rightarrow J/\psi p K^-$ decay modes.

Table S3: The yields, N , and statistical significance, \mathcal{S}_W , of the $\Lambda_b(6146)^0 \rightarrow \Sigma_b^{(*)\pm} \pi^\mp$ and $\Lambda_b(6152)^0 \rightarrow \Sigma_b^{(*)\pm} \pi^\mp$ signals from the fits to the background-subtracted $\Lambda_b^0 \pi^\pm$ mass distributions.

	N	\mathcal{S}_W
$\Lambda_b(6152)^0 \rightarrow \Sigma_b^+ \pi^-$	213 ± 44	7.8σ
$\Lambda_b(6152)^0 \rightarrow \Sigma_b^- \pi^+$	208 ± 43	7.6σ
$\Lambda_b(6152)^0 \rightarrow \Sigma_b^{*+} \pi^-$	163 ± 45	5.3σ
$\Lambda_b(6152)^0 \rightarrow \Sigma_b^{*-} \pi^+$	141 ± 45	4.5σ
$\Lambda_b(6146)^0 \rightarrow \Sigma_b^+ \pi^-$	53 ± 30	2.3σ
$\Lambda_b(6146)^0 \rightarrow \Sigma_b^- \pi^+$	0 ± 20	—
$\Lambda_b(6146)^0 \rightarrow \Sigma_b^{*+} \pi^-$	285 ± 51	8.4σ
$\Lambda_b(6146)^0 \rightarrow \Sigma_b^{*-} \pi^+$	227 ± 52	6.3σ